Land cover-adjusted index for the former Aral Sea using Landsat images

Ilhomjon Aslanov[1*], *Sayidjakhon* Khasanov[1,3], *Yakhshimurad* Khudaybergenov[2], *Michael* Groll[4], *Christian* Opp Ch[4], *F.* Li[3], and *Ramirez* Del-Valle E[5]

[1]Tashkent Institute of Irrigation and Agricultural Mechanization Engineers, Tashkent, Uzbekistan
[2]Department of Geodesy, cartography and natural resources, Karakalpak State University, Nukus, Karakalpakstan, Uzbekistan
[3]Institute of Geographical Sciences and Natural Resources Research, Chinese Academy of Sciences, Beijing, China
[4]Faculty of Geography, Philipps-Universität Marburg, Germany
[5]Institute of Biology, National Autonomous University of Mexico, Mexico

Abstract. The Aral Sea was the fourth largest inland lake on the globe until 1960, with a surface area of about 68,000 km2. Mainly, the huge irrigation projects in many parts of its transboundary catchment were responsible for the catastrophic desiccation and ecological crises of the Aral Sea after second part of 20th century. Ecological crisis surrounding the Aral Sea (lake) regions is one of the critical environmental problems of Central Asia. As a result, monitoring of desertification processes and determining the aerosol concentration in the atmosphere are highly relevant for any attempts to mitigate environmental changes in the Aral Sea basin. Remote sensing is the most appropriate method for studying desertification and dust storms as it easily covers large areas with a high spatial and temporal resolution. Satellite images provide detailed multispectral information about the earth's surface features, which proves invaluable for the characterization of vegetation, soil, water, and landforms at different scales. Vegetation cover, biomass, and soil properties were analyzed with remote sensing methods (NDVI, SDVI). It is emphasized that vegetation indices have little sensitivity at low leaf area which is common to all desert ecosystems.
Keywords: Aral Sea, Water shrinkage, Land-Cover, Remote Sensing, GIS, Central Asia, NDVI

1 Introduction

The immediate cause of the lake water disappearance of the Aral Sea is the fact that its two major rivers, the Amu Darya and Syr Darya, only contributed an average of 5 km³ of water to the lake's annual water balance instead of the former quantity of 56 km³. Besides that, in many years, the river water did not even reach the lake at all [12, 47]. Since there was no sufficient water to ensure the lake water balance, the evaporation rate from shallow

*Corresponding Author: ilhomaslanov@tiiame.uz, ilhomaslanov@gmail.com

depths of the lake has been dramatically increasing, thus urging to actively develop potential remediate measures to combat with this human-induced environmental issue [30, 33, 18, 14]. Detailed analysis of land cover using remote sensing data in large area provides a complete profile for better analyzis and mapping. Instead the lake surface a new desert has been covering the Aral Sea region during the last six decades. Sand and dust storms often do have its source area from this bare sandy area of the Aral Sea accelerating desertification processes [45, 3]. They are often reflecting an early warning about the ongoing local and regional environmental changes around the Aral Sea [46, 5]. Once they progress from slight to serious and severe categories they contribute to the spread of desertification through the transport and deposition of sediments that can destroy local ecosystem and infrastructure, and render areas uninhabitable [43, 30]. During sand transportation, airborne dust is involved in many physicochemical processes of the atmosphere, hydrosphere, and geosphere. Atmospheric sand deposition composes Aeolian mineral particles which strongly contribute to the composition of the sediments, both on the continents and in oceans worldwide [11, 39]. Conducted an in-depth and systematic analysis of long-term space and time variations in of both area and water volume of the Aral Sea, and their potential drivers, which was lacking prior to these experiments[47, 42, 28, 9, 26]. Firstly, they extracted the lake surface area of the Aral Sea using one of the Remote Sensing (RS) indices, Normalized Difference Vegetation Index (NDVI), based on the dataset captured by MODIS during 2000-2018. This extraction enabled to quantify and distinguish the inter-annual variations of lake surface area and water volume of the Aral Sea during 1960–2018 based on long-term hydrological data generated by the MODIS sensor. The results of these experiments revealed that from 1960 to 2018 the area of the Aral Sea shrank dramatically and the average water shrinkage rate per annum accounted for around 1,000 km^2. They claim that this shrinkage rate has decelerated over recent years. Besides that, during the experiments, marginal expansion of the Aral Sea lake surface area was observed. As these scientists assert that in 1986, the Aral Sea split into two lakes. Since then, these two lakes have encountered opposing trends: the much bigger South Aral Sea located in Uzbekistan has shrunk dramatically despite having some trend oscillations, while the North Aral Sea located in Kazakhstan has enlarged obscurely [1].

Considering the above mentioned results, this paper aims to provide an improved insight to spatio-temporal land-cover change, aligning with water shrinkage, from 1960 in the Aral Sea was change water balance and start shrinking but however in the last two decades and to determine a water shrinkage rate per annum based on Landsat sensor. Besides that, as an objective of this paper, once a water shrinkage rate has been ascertained, performing a simplified correlation analysis between land-cover change of the Aral Sea and climate data is contemplated. Based on the expected results some conclusions should be given regarding the water shrinkage effects both on the land use changes and on the formation of sand and dust storms.

2 Study area

Central Asia is the largest landlocked region in the world. The majority part of its landscapes is desert, semi-desert, dry steppes, and high mountains [32]. Due to the fact that the Aral Sea region became after the desiccation disaster of the Aral Sea a very vulnerable ecological zone, where desertification processes have been accelerated during the last four - six decades [24], this study site was selected for further investigations. The Aral Sea is located in the central part of Turan lowland in Central Asia and surrounded by several deserts, and is sandwiched between two deserts, the Karakum and the Kyzylkum. [41, 15] (Fig 1). The Aral Sea is nowadays considered as a salty lake bestriding the Uzbek-Kazakh border, covering an area of approximately 68,478 km^2 with a total volume of 1,064 km^3, a

maximum depth of 69 m, an average depth of 16 m and a shoreline stretching for more than 4,430 km in 1960 [28].

Since the Aral Sea is situated in a dry region with high summer temperatures, where the average annual rainfall is below 250 mm, there is immense evaporation. However, over the past eight decades, annual precipitation in the Aral Sea region has increased, with winter suffering the largest growth trend with 0.7 mm [47]. The Aral Sea region has a distinct continental climate that features exceptionally improved solar radiation and extremely low humidity, negligible rainfall, uncertain time of precipitation, and huge differences between seasonal and annual average temperatures. In the lower locations of this region, average air temperatures in July are around 30 °C while the highest air temperature often reaches 45 °C and 50 °C, respectively; Average air temperatures in the winter season range from −8 °C to 0 °C, with the lowest temperature hovering around −38 °C [4].

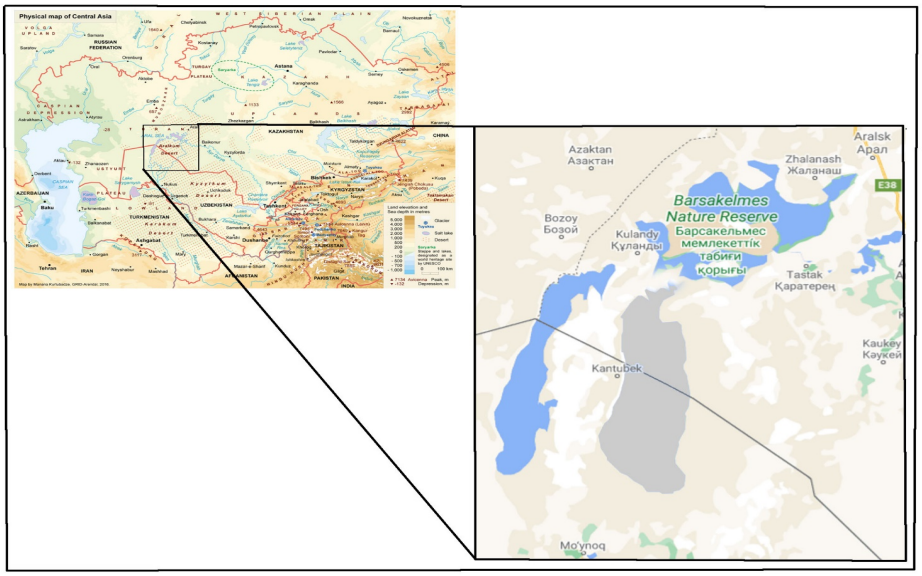

Fig.1**.** Location of the Aral Sea (Source: GRID-Arendal)

3 Methods

Application of remote sensing tools and techniques are important to instantly assess the dynamics of land-cover change at the wider spatial resolution, rather than spending more time on the in-situ research. These tools have a great potential to monitor and evaluate drought processes and water shrinkage including the Aral Sea disaster [17, 41] first started to locate, assess and monitor the land-cover in drylands with geo-information systems (GIS) and RS techniques. They claimed that GIS and RS-based data provide a permanent record of the land-cover changing rate in such a format that records measurable changes. [17] considered that the RS approach towards the land cover analysis plays an important and key role as one of the major sources of state-of-the-art and physically-based information, whereas GIS provides the toolbox that improves the ability of data integration, data analysis and data extraction from the source. According to [2, 7, 25, 36] it is possible to understand the desertification rate as a result of land-cover changes. The amounts of land-cover changes can be assessed by using RS indices like NDVI and Soil-Adjusted Vegetation Index (SAVI). These indices might function as a basis for an early warning of

desertification. NDVI and SAVI, calculated using satellite images, have revealed the capability of RS for systematic, reliable and spatially extensive monitoring of drought after water shrinkage [7, 29, 37, 38]. Recent studies have also shown that with the help of the integrated use of GIS and RS analyses of both temporal and spatial dynamics of land-cover changes caused by drying surface water bodies become possible, [46] analyzing potential changes occurring among land cover features and develop the baseline maps of desertification or land-cover [6, 16, 44]. Concerning these studies, RS implies either satellite images or aerial photography to perform a trend analysis for future scenarios and create trend maps showing the possible changes in land cover condition over a certain period [27].

4 Data

The Physical map of Central Asia from 1960 was taken as a source to extract the former extent of the Aral Sea, which was 68,000 km^2, to gain a deep insight how land-cover of this region has spatially and temporally changed in combination with water shrinkage. However, the base year of the present analysis is set in 1999, because the nationwide assessment of the Aral Sea shrinkage effects was commenced, and the analysis was conducted till 2019. This Physical Map was digitized in order to extract the borders of extent of the Aral Sea for further analysis.

For secondary data satellite images taken especially in the end of each year (1999, 2009, and 2019) were downloaded from the open source databases Earth Explorer and Glovis (www.earthexplorer.usgs.gov; www.glovis.usgs.gov). This period was used to learn similar patterns at the end of the years. For this reason, the last cloud-free days of December are highly appropriate to observe the dynamics of land-cover in the Aral Sea region. Regarding the sensors of satellite images, Landsat TM 5, Landsat ETM+ 7 and Landsat 8 OLI (for further information on Landsat sensors, see CRISP) were used. The temporal resolution of the selected sensors is 16 days, whereas, the spatial resolution of images is 30 meters, which means one pixel of the image covers 30 m x 30 m of land surface.

4.1. Data processing and analysis

The analysis of land-cover in the shrinking Aral Sea region required several steps to interpret the results. Firstly, initial preprocessing steps and operations on satellite images (e.g. atmospheric and geometric corrections, outlier removal and mosaicking) were undertaken which directly improved the quality and the accuracy of the remote sensing maps [38, 25, 23, 21, 8]. Then the further analysis was conducted by using ArcGIS and Erdas Imagine software packages. Then, a GIS tool called “Resample” was used in order to convert the actual pixel size of the satellite images to 150 meters x 150 meters to expedite analyzing processes, return an enhanced visualization, and reduce the size of the remote sensing images to ensure proper data storage. Afterwards, the Normalized Difference Vegetation Index (NDVI) was applied to detect the canopy cover from the satellite images. The NDVI ranges from -1 to 1 and assesses whether the target being analyzed contains photosynthetically active vegetation or not by using Equation 1 [2]:

$$NDVI = \frac{NIR-RED}{NIR+RED} \quad (1)$$

Where: NIR is the Near InfraRed band of Landsat sensor (band 4 for Landsat TM 5 and Landsat ETM+ 7; band 5 for Landsat 8 OLI); and RED is the red band of Landsat sensor (band 3 for Landsat TM 5 and Landsat ETM+ 7; band 4 for Landsat 8 OLI).

Once the NDVI was calculated, vegetation cover above 0.3 NDVI was removed from each satellite image [22, 35] in order to improve the accuracy of the Soil-Adjusted Vegetation Index (SAVI) values ranging from -1.5 to 1.5. The SAVI enables the sufficient description of the soil-vegetation system and soil type classification which is essential for estimating the consequences of land-cover change by using Equation 2 [19, 2].

$$SAVI = \frac{NIR-RED}{NIR+RED+L} \times (1 + L) \quad (2)$$

Where: L is a soil adjustment factor (according to Huete (1988), L = 0.5)

After all, the NDVI and SAVI-based maps were stacked to create final land-cover maps. When a potential RS index, SAVI, was found to describe the soil system and reflection, the footprint (to verify whether sandy soil or vegetation cover is dominantly occupying the Aral Sea region) of water shrinkage in the Aral Sea was evaluated for all years (1999-2019).

When outcome maps were created for all years, the dynamics of the salt-sand-canopy cover close to the study area were showing whether the actual area of the lake was preoccupied by canopy or bare (salty-)sandy soil. As far as the actuality was identified, the above-mentioned step-by-step methods were enough to tell the average annual water shrinkage rate of the Aral Sea.

A simple correlation analysis was performed using R software to identify how water shrinkage correlated with wind speed and air temperature. Data on wind speed and air temperature were recorded in two different meteo-stations, ‘Aralskoe More’ and ‘Uyaly’, located close to the Aral Sea and were retrieved from an open source “NASA Earth Observatory”. Additionally, for statistically proving the correlation between wind speed and water shrinkage, a simple linear regression analysis was undertaken to check whether the p-values of all variables were statistical significant ($p > 0.05$ – statistically insignificant; $p < 0.05$ – statistically significant).

5 Results

As a consequence of the drying up of the Aral Sea for the last 20 years, the landscape of the dried-up part of the Aral Sea was completely transformed, thus a new born desert – Aral-Kum desert appeared **(Fig 2)**. New map of Aral-Kum illustrates the land-cover map of the study area for the last two decades.

According to the land-cover maps **(Fig. 2)** created by the combination of NDVI and SAVI indices, already visually, the lake surface area of the Aral Sea has experienced a critical shrinkage. On the other hand, aligning with sandy areas, salty sand areas have dramatically extended to the eastern side and, over decades, due to natural phenomena, salty sand has also migrated from the east to the central part. It is interesting to note that the of mud and vegetation areas were still not preoccupied by hazardous sandy or salty layers. Thereafter, in order to derive quantitative values on the distribution of each land-cover class, the “Reclassify” operation was performed in ArcGIS software to transfer the qualitative data into quantitative. The result of this operation is displayed in (**Fig. 3)**.

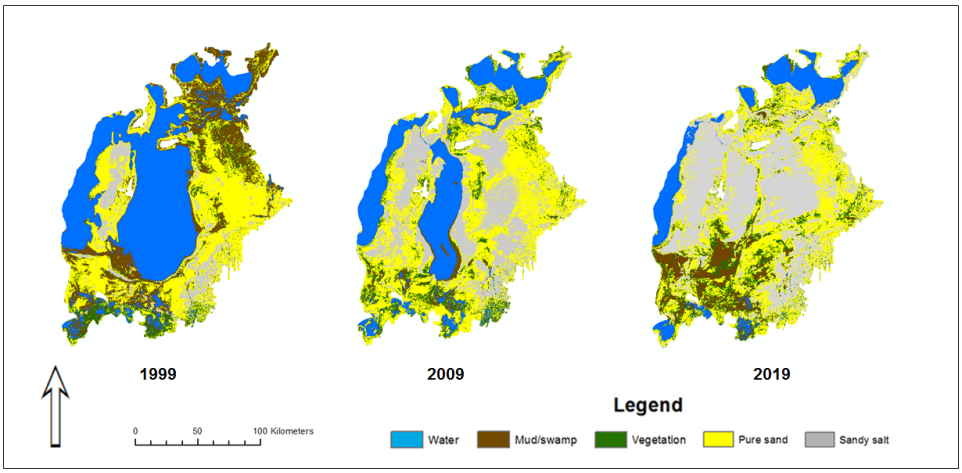

Fig. **2.** Dynamics of land-cover change in the Aral Sea from 1999 to 2019.

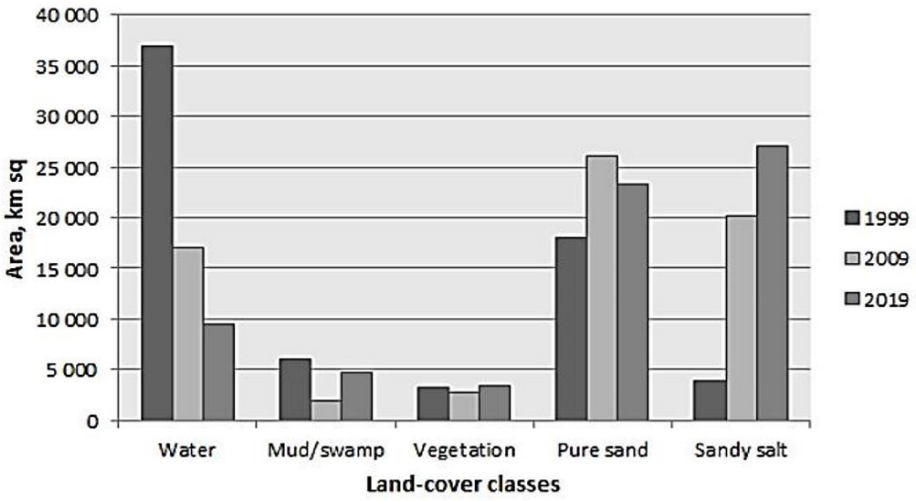

Fig. 3. Breakdown of land cover classes from 1999 to 2019

As can be seen in Fig. 3, there were evidentially upward trends for the extension of the actual sandy salt and sandy areas, despite experiencing fluctuations. Sandy areas occupied approximately 18,000 km^2 in 1999, whereas sandy salt areas accounted for below 5,000 km^2. Both land-cover classes have invaded another roughly 5,000 km^2 and 20,000 km^2 of the Aral Sea territory, respectively, by the end of 2019. The lake area sharply has been shrunk by approximately 25,000 km^2 over 20 years. However, the other two land-cover classes, mud and vegetation cover, almost remained stable in the entire period of the analysis, where vegetation cover in the Aral Sea region was rather certain than muddy area.

Referring to Figure 3 it is possible to calculate the average shrinkage value. Compiling all of the enlarged and decreased land-cover areas together, the annual water shrinkage rate per annum of 1,372.65 km^2 was determined.

After having calculated the shrinkage rate, a simple correlation analysis was carried out for water and all land-cover classes to understand how the changes in each class interconnected each other (Table 1).

Table 1. Correlation analysis of land cover classes

	Water	Mud/Swamp	Vegetation	Pure sand	Sandy salt
Water	1	0.66	0.59	-0.99	-0.99
Mud/Swamp	0.66	1	0.74	-0.91	-0.65
Vegetation	0.59	0.74	1	-0.46	0.01
Pure sand	-0.99	-0.91	-0.46	1	0.80
Sandy salt	-0.99	-0.65	0.01	0.80	1

According to the interesting aspect of the correlation table (Tab. 1), water was positively correlated with mud (0.66) and vegetation (0.59). More specifically this means, when lake surface area increases, mud and vegetation will stay proportional as a response to the increase of lake surface area. However, the lake surface area was totally and negatively correlated with pure sand (-0.99) and sandy salt (-0.99) causing an increase when lake area shrinks.

For the continuation of the statistical analysis, ANOVA was applied for water areas to check its dynamics and the shrinkage whether it was significant or not. As a result, R^2 was equal to 0.83 in three observations, whereas F and F critical were 3.532 and 3.478, respectively, according to the results of ANOVA (Table 2). Last but not least, the p-value was calculated to test against statistical significance of water shrinkage rate in relation with other land-cover classes. The p-value here is the main character of the table, indicating if the relation between variables is statistically significant ($p > 0.05$ – insignificant; $p < 0.05$ – significant).

Table 2. ANOVA output

Source of variation	SS*	df**	MS***	F ratio	p-value	F critical
Between groups	1.04E+09	4	2.59E+08	3.532	0.0028	3.478
Within groups	7.34E+08	10	7.34E+07			
Total	1.77E+09	14				

*-sum-of-square – sum of the square of variation;
**-degree of freedom – the maximum number of logically independent values (in our case, the water shrinkage rate of the Aral Sea) that have the freedom to vary;
***-mean squares – an estimate of population variance;

Once the correlation between classes was revealed, the correlation between such land-cover classes (lake, pure sand and sandy salt) and climate factors was founded to determine the role of wind speed and air temperature for water shrinkage and for the formation of sand and dust storms.

As emphasized in the methodology, climate data like wind speed and average seasonal air temperature in summer were additionally included in the correlation analysis for such land-cover classes (Table 3).

Table 3. Correlation coefficients between climate factors and land-cover classes

		Water	Pure sand	Sandy salt
'Aralskoe More' meteostation	avg. T, °C	-0.91	0.52	0.93
	WS, m/s	-0.86	0.99	0.84
'Uyaly' meteostation	avg. T, °C	-0.94	0.96	0.93
	WS, m/s	-0.98	0.90	0.98

According to the data presented in Table 3, in general, there is a huge impact of climate data on water shrinkage and these two climate factors boost the actual evaporation rate. Herein, a decrease of lake area in the Aral Sea region was exceptionally and significantly correlated with wind speed and seasonal average air temperature registered in two different meteostations close to the study area. As the main primary or natural drivers of ecosystem destruction and dust and sand storms formation in the region, these climate factors were seriously correlated with pure sand and sandy salt which can migrate through wind due to their minor particle size.

Referring to the correlation tables, it is assumed that the impact of climate factors was mainly detected and significantly relevant to the change in lake surface area. While an increase in air temperature leads to an adverse change in lake areas as a result of evaporation, it can be assumed that the current policies for regional climate action need to be sustainably amended.

6 Conclusions

This paper shows that as a result of the drying up of the Aral Sea over the last 20 years, a new salty desert, namely Aral-Kum desert, has formed on an extensive area in its dried part. As the Aral Sea shrinking water is replaced by newly formed salty desert, known as Aral-Kum, the potential for the mobilization of salts and heavy metals included in the exposed lake sediments raises considerable concerns for the southern Aral Sea region, which is mainly affected by dust from the Aral-Kum. Most of the Aral-Kum sediments show negligible heavy metal concentrations, indicating that the Aral Kum might not be the major source of these pollutants, but that local geological and anthropogenic factors are prevalent. The high variability of both spatial and temporal dust deposition intensity, the grain size of the chemical composition of the dust [32] leads to the conclusion that continuous on-site monitoring is needed for a competent understanding of the dust translocation processes in the densely populated areas of the southern Aral Sea region, their impact on the human health, and their effects to the intensely used land. This research is very cost-effective and easy to maintain so that a continuation of this long-term ecological monitoring is feasible, even during times of financial restrictions.

References

1. N. V. Aladin. W. T. W. Potts. Changes in the Aral Sea ecosystem during the period 1960-1990. Hydrobiologia. (1992)
2. A. Bannari. D. Morin. F. Bonn. A.R. Huete. A review of vegetation indices. Remote Sensing Reviews, **13**(1-2), 95-120. (1995)
3. A. Burton. Northern Aral Sea Filling up Fast. Frontiers in Ecology and the Environment, Vol. **4**, No. **5**. http://www.jstor.org/stable/3868774 (2006)
4. CAWATERinfo. The Aral Sea Basin. Available online from http://www.cawater-info.net/aral/index_e.htm/Accessed 13 August (2018)
5. E.J. Crighton. Barwinl. I. Small. R. Upshur. What have we learned? A review of the literature on children's health and the environment in the Aral Sea area. Int J Public Health (2011)
6. S. I. Deliry. Z. Y.Avdan. N. T.Do. U Avdan. Assessment of human-induced environmental disaster in the Aral Sea using Landsat satellite images. Environmental Earth Sciences. (2020)

7. A. Diouf. E.F. Lambin. Monitoring land-cover changes in semi-arid regions: remote sensing data and field observations in the Ferlo, Senegal. Journal of Arid Environments, **48(2)**, (2001)
8. D. V. Fedorov, L. M. G. Fonseca, C. Kenney, B. S. Manjunath. Automatic registration and mosaicking system for remotely sensed imagery. In Image and Signal Processing for Remote Sensing VIII Vol. **4885**. (2003)
9. B. Gaybullaev, S.C Chen, D. Gaybullaev. Changes in water volume of the Aral Sea after 1960. Appl. Water. Sci. **2 (4)**. https://doi.org/10.1007/s13201-012- 0048-z (2012)
10. M. H. Glantz Aral Sea Basin: A Sea Dies, a Sea Also Rises. Ambio, Vol. 36, No. **4** http://www.jstor.org/stable/4315834 (2007)
11. L. Gomes and A. Gillette A comparison of characteristics of aerosol from dust storms in Central Asia with soil-derived dust from other regions. Atmospheric Environment Vol. **27A**, No. 16. (1992)
12. B. Grobety et al. Airborne particular in the urban Environment. *Elements.* Vol. No **6**. (2010)
13. M. Groll et al. Long term analysis of Aeolian dust in Central Asia – Results from the CALTER-Project. In: Marburg International Dust & Sand Storm (DSS) Symposium "DSS and Desertification". (2009)
14. M. Groll. Chr. Opp. I. Aslanov. Spatial and Temporal distribution of the dust deposition in Central Asia – results from a long term monitoring program. Aeolian Research, Elsevier, DOI: 10.1016/j.aeolia.2012.08.002 (2012)
15. M. Groll. Ch. Opp. G. Issanova. N. Vereshagina,O. Semenov. Physical and Chemical Characterization of Dust Deposited in the Turan Lowland (Central Asia). Central Asian Dust Con. Vol. **99**. DOI: https://doi.org/10.1051/e3sconf/20199903005 (2009)
16. T. Higginbottom., E Symeonakis. Assessing land degradation and desertification using vegetation index data: Current frameworks and future directions. *Remote Sensing*, **6(10)**, (2014)
17. P.Hostert. A. Roder. T. Jarmer. T. Udelhoven. J. Hill. The potential of remote sensing and GIS for desertification monitoring and assessment. *Annals of Arid Zone,* **40(2)**, (2001)
18. X. Huang et al. Dust deposition in the Aral Sea: implication for the changes in atmospheric circulation in central Asia during the past 2000 years. In: *Quaternary Science* reviews. (2011)
19. A. R. Huete, A. R. A soil-adjusted vegetation index (SAVI). *Remote sensing of environment*, **25(3)** (1988)
20. R. Indoitu, L. Orlovsky, N. Orlovsky. Dust storms in Central Asia: Spatial and temporal variations. *Journal of Arid Environments,* **85** (2012)
21. R. R. Irish, J. L. Barker, S. N. Goward, T Arvidson,. Characterization of the Landsat- 7 ETM+ automated cloud-cover assessment (ACCA) algorithm. *Photogrammetric engineering & remote sensing,* **72(10)** (2006)
22. K. Ivushkin, H. Bartholomeus, A. K. Bregt, A. Pulatov. Satellite thermography for soil salinity assessment of cropped areas in Uzbekistan. *Land degradation & development,* **28(3)** (2017)
23. N. G. Kardoulas, A. C. Bird, A. I. Lawan, Geometric correction of SPOT and Landsat imagery: a comparison of map-and GPS-derived control points. *Photogrammetric Engineering and Remote Sensing,* **62(10)** (1996)

24. K. L. Kiessling Conference on the Aral Sea: Women, Children, *Health and Environment. Ambio*, Vol. **27**, http://www.jstor.org/stable/4314791(1998)
25. S. Liang, H. Fang, M. Chen. Atmospheric correction of Landsat ETM+ land surface imagery. I. Methods. *IEEE Transactions on geoscience and remote sensing*, **39(11)**, (2001)
26. P. N. Makkaveev, V. V. Gordeev, P. O. Zav'yalov, A. A. Polukhin, P. V. Khlebopashev A. I. Kochenkova. Hydrochemical characteristics of the Aral Sea in 2012–2013. *Water resources*, **45(2),** (2018)
27. M. Masoudi, P. Jokar, B. Pradhan. A new approach for land degradation and desertification assessment using geospatial techniques. *Natural Hazards and Earth System Sciences*, **18(4)**, (2018)
28. P. Micklin. The future Aral Sea: hope and despair. *Environmental Earth Sciences*, **75(9)**, (2016)
29. S. E. Nicholson, C. J. Tucker, M. B Ba. Desertification, drought, and surface vegetation: An example from the West African Sahel. *Bulletin of the American Meteorological Society*, **79(5)** (1998)
30. Chr Opp. Desertification in Uzbekistan. Geographische Rundschau International Edition Vol. **1, 2**: (2005)
31. Chr.Opp, Vom Aralsee zur Aralkum: Ursachen, Wirkungen und Folgen des Aralseesyndroms. Asien (Reihe Planet Erde). (2007)
32. Chr.Opp, M. Groll, I. Aslanov, T. Lotz, N.Vereshagina. Aeolian dust deposition in the Southern Aral Sea region (Uzbekistan) ground base monitoring results of LUCA project. Quaternary International **429**, (2017)
33. Ch.Opp, M. Groll, O. Semenov, N. Vereshagina,A. Khamzina. Impact of the Aral Sea Syndrome – the Aralkum as a Man-Made Dust Source. E3S Web of Conferences **99** https://doi.org/10.1051/e3sconf/20199903003 (2019)
34. L. Orlovsky, G. Tolkacheva, N. Orlovsky, B. Mamedov. Dust storms as a factor of atmospheric air pollution in the Aral Sea basin. *WIT Transactions on Ecology and the Environment*, **74**. (2004).
35. A. Platonov, A. Karimov, S. Prathapar. Using satellite images for multi-annual soil salinity mapping in the irrigated areas of Syrdarya province. Journal of Arid Land Studies, **25-3** (2015)
36. S Prince. Mapping desertification in southern Africa. In: Land Change Science: Observing, Monitoring, and Understanding Trajectories of Change on the Earth's Surface (Gutman G, Janetos A, Justice CO, Moran EF, Mustard JF, Rindfuss RR, Skole D, Turner II BL, eds), pp. 163-184. Kluwer, Dordrecht, NL. (2004).
37. S. D. Prince, C. O. Justice. Coarse resolution remote sensing of the Sahelian environment. Ecology and Society, **13(7)** (1991)
38. R. Richter. A fast atmospheric correction algorithm applied to Landsat TM images. Title Remote Sensing, **11(1)** (1990)
39. K. Schepanski. Transport of mineral dust and its impact on climate. Geosciences **8, 151** doi:10.3390/geosciences8050151(2018)
40. I. V. Severskiy Water-Related Problems of Central Asia: Some Results of the (GIWA) International Water Assessment Program. *Ambio*, Vol. **33**, No. 1/2, Transboundary Issues in Shared Waters http://www.jstor.org/stable/4315455 (2004)
41. A. S. Walker, C. J. Robinove, Annotated bibliography of remote sensing methods for monitoring desertification (No. 851). US Geological Survey. (1981)

42. X. Wang. Y. Chen, Z. Li, G. Fang, F.Wang, H. Liu, The impact of climate change and human activities on the Aral Sea Basin over the past 50 years. Atmospheric Research, **245**, (2020)
43. G. F. S.Wiggs, S. L.O'hara, Wegerdt, J. Van Der Meer, I. Small, R. Hubbard. The Dynamics and Characteristics of Aeolian Dust in Dryland Central Asia: Possible Impacts on Human Exposure and Respiratory Health in the Aral Sea Basin. The Geographical Journal, Vol. **169**, No. 2 (2003) http://www.jstor.org/stable/3451395.
44. T. Wu, S. Sang, S. Wang, Y. Yang, M. Li, Remote sensing assessment and spatiotemporal variations analysis of ecological carrying capacity in the Aral Sea Basin. Science of The Total Environment, (2020).
45. I. Ying et al. Characterization of Asian dust storm and non-Asian dust storm PM2.5 aerosol in southern Taiwan. Atmospheric Environment **40** (2006)
46. H. Yongxiang et al. Dust storm in Asia continent and its bio-environmental effects in the North Pacific: A case study of the strongest dust event in April, 2001 in central Asia. *Chinese Science Bulletin* Vol. **51** (2006)
47. X. Yang, N.Wang, J.He, T.Hua, Y. Qie. Changes in area and water volume of the Aral Sea in the arid Central Asia over the period of 1960–2018 and their causes. CATENA, **191** (2020)